

Theoretical Analysis of Human Rhythmic Jumping on Oscillating Floors

Phablo V. I. Dias^{1,2}, Zenón J. G. N. del Prado¹

¹*School of Civil and Environmental Engineering, Federal University of Goiás
Avenida Universitária, 1488, Setor Leste Universitário, 74605-200, Goiânia, GO, Brazil
phablo@discente.ufg.br, zenon@ufg.br*

²*Dept. of Civil Engineering, Federal Institute of Science and Technology of Tocantins
Alameda Madrid, 545, Setor Jardim Sevilha, 77410-470, Gurupi, TO, Brazil
phablo.dias@ifto.edu.br*

Abstract. This study investigates the dynamic interaction between a human jumper and a concrete rectangular plate under cyclic vertical jumps. The plate is described using Von Kármán's nonlinear relations, while the jumper is modeled as a spring-mass-damper (SMD) system with a harmonic force acting on the human's center of mass to represent the propulsion force during jumping. The mechanical system is described by a set of piecewise smooth-touch nonlinear differential equations, allowing the loss of contact between the jumper and the plate during jumps. The results show that the jumper exhibits complex dynamics, including periodic and chaotic responses, depending on the system's parameter combinations. Additionally, the SMD model can affect the mechanical behavior of the plate by coupling the jumper's vibration modes with the structure's, creating new resonance frequencies and redistributing the vibrational energy.

Keywords: Human-Structure Interaction, Nonlinear Dynamics, Rectangular Plates.

1 Introduction

Loads resulting from rhythmic human activities such as walking, running, dancing, and jumping are commonly observed in structures like walkways, floors of buildings with large spans, and grandstands. These activities are often prompted by visual and/or auditory stimuli, particularly in environments such as dance clubs, concert halls, fitness centers, and stadiums during sporting events. Before understanding the interactions between humans and structures, particularly regarding induced structural vibrations, it is essential to rigorously study and characterize the behavior of the human body during activity and the consequent loads applied to the structure. The characterization these loads is complex, as various factors influence them, including individual characteristics such as gender, weight, age, physical fitness, and the manner of performing the activity. Furthermore, these loads can be classified based on the direction of body movement and motor execution, directly affecting how body mass is projected [1].

For instance, in walking, running, and oblique jumps, the displacements and velocities of the human body over time are analyzed in two components: vertical and horizontal. The vertical component results from leg flexion, while the horizontal component is due to the individual's movement on the plane. Conversely, for vertical jumps, only one component is considered since the movement predominantly occurs along the vertical axis, with minimal horizontal displacement. Moreover, a distinction is made between human movements where the feet maintain full contact with the structure and those where contact is lost. During walking, for example, it can be assumed that at least one foot remains in contact with the structure at all times, unlike in jumping, where the feet momentarily lose contact. As shown in Figure 1, rhythmic vertical jumps can be decomposed into flight and contact phases, during which human and structural behavior may change.

The contact phase begins with preparation, where the jumper lands and prepares for the jump. This is followed by the propulsion period, which is subdivided into compression (loading) and extension (unloading) stages. In the compression stage, the jumper flexes their knees, accumulating energy. In the extension stage, the knees extend, releasing energy and resulting in take-off. According to Ref. [2], human biodynamic properties, such as the stiffness of the lower limbs, can vary between these stages. After take-off, the individual enters free fall until touch-down, restarting the preparation period. Depending on the propulsion force and system parameters, decoupling may not occur or may be negligible due to low jump amplitude. This movement, with no significant

loss of contact, is known as bobbing or bouncing. A complete jumping period (T) is the sum of contact time

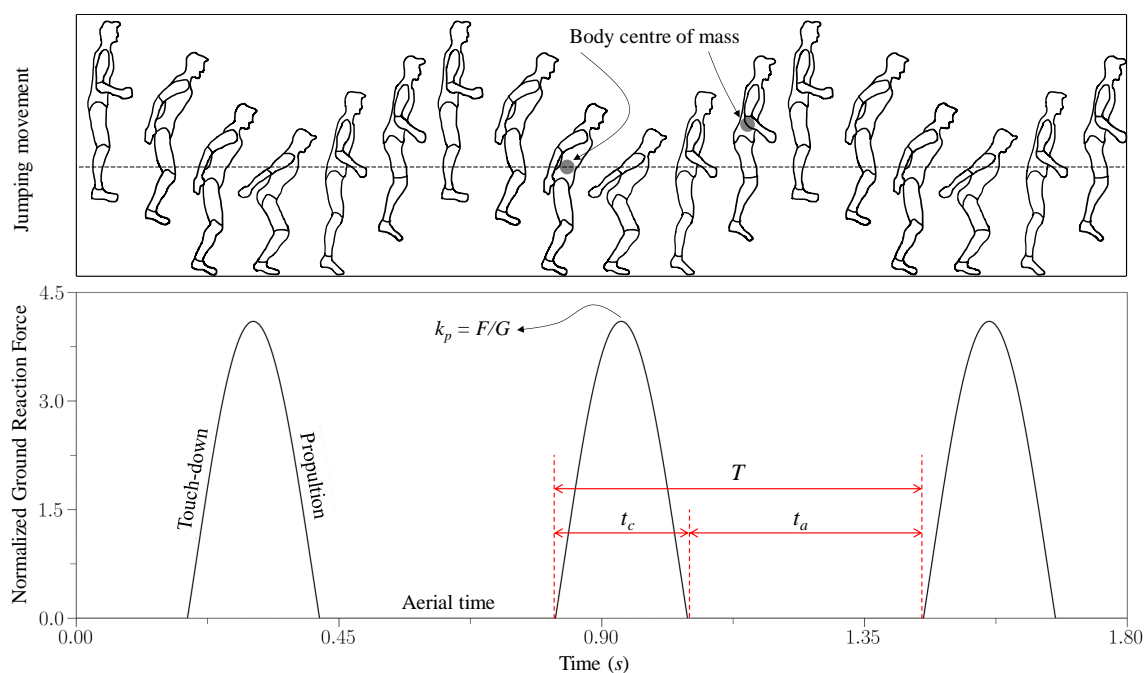


Figure 1. Human movement during rhythmic vertical jumps [Adapted from [3]].

(t_c) and aerial time (t_a). Thus, the coefficient $\alpha_C = t_c/T$ estimates the proportion of the contact period in the rhythmic jump period. Ref. [4] found that α_C varies with jump frequency and averages around 0.63. For bobbing, these values are indistinguishable due to full foot contact with the floor. Additionally, it has been observed that leg stiffness can change depending on the chosen jump frequency, exhibiting nonlinear behavior.

Another important aspect is the maximum impact factor (k_p) applied to the floor, given by the ratio of the reaction force on the structure to the individual's body weight. This factor depends on the jump excitation frequency, as individuals adapt their biodynamic parameters to maintain balance and periodicity. Normalized force values (k_p) exceeding 5 may be physiologically unacceptable, potentially causing knee injuries [5]. When the normalized force response (k_p) peaks, the body's center of mass (C.O.M) displacement is minimal, and velocity is zero, indicating the limit of knee flexion. At takeoff, the velocity reaches a maximum, then decreases against gravity.

During the flight period, when the displacement of the center of mass reaches a maximum, the velocity returns to zero. Generally, time responses for displacements and velocities are phase-shifted by $\pi/2$. The velocity shows a linear variation during flight, graphically resembling shark teeth. Body movement is often characterized by accelerometers positioned in the lumbar spine region, where the center of mass is located [6, 7].

Experimental studies indicate that humans can jump at frequencies from 1.5 to 3.5 Hz on slightly oscillating or rigid floors [8–10], with 2.0 Hz being more comfortable for groups without a fixed jump frequency target [4]. Although dominant harmonics exist in evaluating jump frequencies, experimental responses tend to show energy leakage to adjacent harmonics.

This indicates that human movement on floors during jumps may not be periodic, depending on system parameters, especially in more oscillating systems prone to interaction. This interaction is influenced by intra-variability, the individual's ability to vary their biodynamic properties as jump frequency changes, aiming for a more comfortable movement. In the works of Ref. [11, 12], it was observed that duplications of the body's center of mass oscillation period can occur at lower jump frequencies. Quasi-periodic solutions, chaotic sections, and coexistence of attractors can also be found in oscillating floors, indicating the difficulty or impossibility of orderly jumping under certain conditions.

This study analyzes the dynamic interaction between a human jumper and a concrete rectangular plate subjected to cyclic vertical jumps. The plate's behavior is modeled using von Kármán's nonlinear relations, while the jumper is represented as a spring-mass-damper (SMD) system with a harmonic force acting on its degree of freedom to simulate the propulsion force acting on the human center of mass during jumping. The mechanical system is governed by a set of piecewise smooth-touch nonlinear differential equations, accounting for the intermittent contact between the jumper and the plate.

2 Mathematical Model

The mathematical model considers the jumper as a mass-spring-damper (SMD) oscillator with one degree of freedom and modal mass m_h , an equivalent leg stiffness k_h , and a damping coefficient c_h . The floor is represented by a simply supported rectangular plate described by Kirchhoff-Love theory, with displacement fields u , v , and w , dimensions a and b , thickness h , density ρ , and Young's modulus E , as studied by [12]. In formulating the problem, Lagrange's equation is utilized. It is assumed that the potential energy (U) and kinetic energy (T) of the system are coupled, given by the sum of the jumper's energy and the plate's energy, which can be expressed as:

$$U = U_P + U_H; \quad (1)$$

$$T = T_P + T_H; \quad (2)$$

where U_P and T_P are the potential and kinetic energy of the plate, respectively. Similarly, U_H and T_H are the potential and kinetic energy of the jumper, respectively.

Therefore, the potential and kinetic energies of the coupled system can be written as:

$$\begin{aligned} U_P = & \frac{1}{2} \frac{Eh}{(1-\nu^2)} \int_0^a \int_0^b \left(\varepsilon_{x,0}^2 + \varepsilon_{y,0}^2 + 2\nu \varepsilon_{x,0} \varepsilon_{y,0} + \frac{1-\nu}{2} \gamma_{xy,0}^2 \right) dy dx \\ & + \frac{1}{2} \frac{Eh^3}{12(1-\nu^2)} \int_0^a \int_0^b \left(\kappa_x^2 + \kappa_y^2 + 2\nu \kappa_x \kappa_y + \frac{1-\nu}{2} \kappa_{xy}^2 \right) dy dx \\ & + \frac{1}{2} k_h \left(w_h - w(x, y, t) |_{x=x_1, y=y_1} \right)^2; \end{aligned} \quad (3)$$

$$T = \frac{1}{2} \rho h \int_0^a \int_0^b \left(\dot{u}(x, y, t)^2 + \dot{v}(x, y, t)^2 + \dot{w}(x, y, t)^2 \right) dy dx + \frac{1}{2} m_h \dot{w}_h^2. \quad (4)$$

The damping of the plate is assumed to be of the viscous type and is characterized using the Rayleigh dissipation function [13]. In a similar manner, the damping terms for the SMD model are also described by the Rayleigh dissipation function [12]. Consequently, the non-conservative damping forces of the plate F_P and the jumper F_H are given by:

$$F = F_P + F_H; \quad (5)$$

$$\begin{aligned} F = & \xi_p, \omega_{1,1}, m_j \int_0^a \int_0^b \left(\dot{u}(x, y, t)^2 + \dot{v}(x, y, t)^2 + \dot{w}(x, y, t)^2 \right) dy, dx \\ & + \zeta_h, \omega_h, m_h \left(\dot{w}_h - \dot{w}(x, y, t) |_{x=x_1, y=y_1} \right)^2; \end{aligned} \quad (6)$$

where ξ_p , $\omega_{1,1}$, and m_j are the viscous damping ratio, first mode vibration frequency, and modal mass of the plate, respectively. Similarly, ζ_h , ω_h , and m_h refer to the damping ratio, natural frequency, and modal mass of the jumper, respectively.

In this work, a harmonic force is considered acting on the degree of freedom of the SMD model (w_h) to characterize both the compression and propulsion exerted by the jumper during rhythmic jumping movements, as illustrated in Fig. 2. Additionally, the static weight of the jumper ($m_h g$) against gravity is also considered. Thus, the work (W) done by the external forces acting on the SMD model during jumping can be written as:

$$W = w_h (A_h \sin(\Omega, t) - m_h, g) \quad (7)$$

where A_h and Ω are the amplitude and forcing frequency of the propulsion force, respectively; g is the acceleration due to gravity, and w_h and m_h are the displacement and modal mass of the jumper's center of mass, respectively.

The plate is assumed to be simply supported in the vertical direction and has fixed edges in the axial direction, leading to the selection of the following displacement fields $u(x, y, t)$, $v(x, y, t)$, and $w(x, y, t)$ in the axial and transverse directions, which satisfy the boundary conditions.

$$u(x, y, t) = \sum_{m=1}^{M_u} \sum_{n=1}^{N_u} u_{m,n}(t) \sin\left(\frac{m\pi x}{a}\right) \sin\left(\frac{n\pi y}{b}\right); \quad (8)$$

$$v(x, y, t) = \sum_{m=1}^{M_v} \sum_{n=1}^{N_v} v_{m,n}(t) \sin\left(\frac{m\pi x}{a}\right) \sin\left(\frac{n\pi y}{b}\right); \quad (9)$$

$$w(x, y, t) = \sum_{m=1}^{M_w} \sum_{n=1}^{N_w} w_{m,n}(t) \sin\left(\frac{m\pi x}{a}\right) \sin\left(\frac{n\pi y}{b}\right), \quad (10)$$

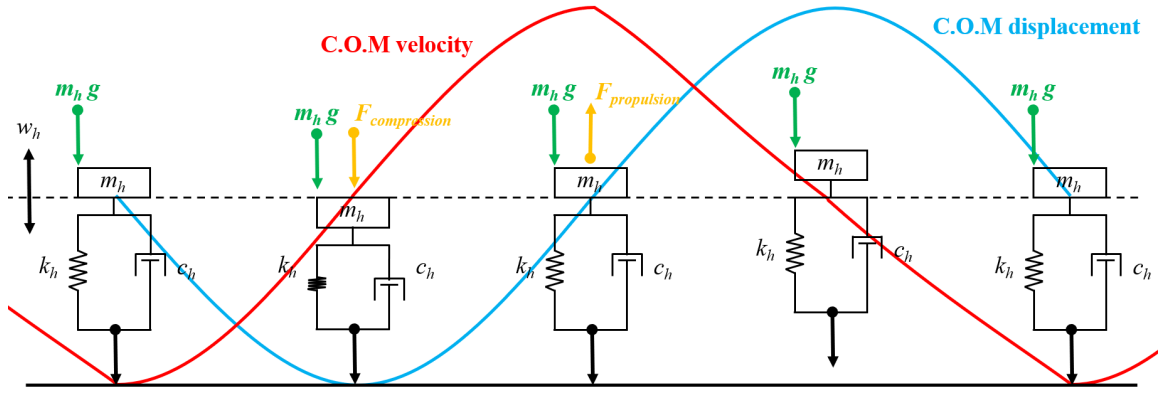


Figure 2. Action of the compression and propulsion force on SMD model during rhythmic vertical jumping.

where m and n are the half-wave numbers in the x and y directions, respectively; M_u , N_u , M_v , N_v , M_w , and N_w are the number of terms used in each displacement field; $u_{m,n}(t)$, $v_{m,n}(t)$, and $w_{m,n}(t)$ are the unknown amplitudes.

Thus, the vector of generalized amplitudes of the coupled plate is given by:

$$\mathbf{q} = [u_{1,1}(t), \dots, u_{M,N}(t), v_{1,1}(t), \dots, v_{M,N}(t), w_{1,1}(t), \dots, w_{M,N}(t), w_h]^T, \quad (11)$$

where its dimension is given by the sum of the number of degrees of freedom considering the displacement fields of the plate ($N_q = N_u + N_v + N_w$) with the degree of freedom of the SMD model. A generic element of the vector \mathbf{q} is referred to as q_i , for $1 \leq i \leq \tilde{N}$, with $\tilde{N} = N_q + 1$.

In order to derive the set of nonlinear dynamic equations, the Rayleigh-Ritz method is employed in conjunction with the Hamiltonian principle [13], which is given as follows:

$$\frac{d}{dt} \left(\frac{\partial \mathcal{L}}{\partial \dot{q}_j} \right) - \frac{\partial \mathcal{L}}{\partial q_j} = Q_j; \quad \text{with } Q_j = \frac{\partial W}{\partial q_j} - \frac{\partial F}{\partial \dot{q}_j}, \quad j = 1..N_q; \quad (12)$$

$$\frac{d}{dt} \left(\frac{\partial \mathcal{L}}{\partial \dot{q}_{\tilde{N}}} \right) - \frac{\partial \mathcal{L}}{\partial q_{\tilde{N}}} = Q_{\tilde{N}}; \quad \text{with } Q_{\tilde{N}} = \frac{\partial W}{\partial q_{\tilde{N}}} - \frac{\partial F}{\partial \dot{q}_{\tilde{N}}}, \quad \tilde{N} = N_q + 1; \quad (13)$$

where \mathcal{L} represents the Lagrangian function, defined as $\mathcal{L} = T - U$. The equations involve generalized forces denoted by Q_j for $1 \leq j \leq N_q$ and $Q_{\tilde{N}}$ for $\tilde{N} = N_q + 1$.

Then, the nonlinear equations of motion of the coupled system shown in (12) and (13) can be written as:

$$m_j \ddot{q}_j + \sum_{i=1}^{N_q} c_{j,i} \dot{q}_i + \sum_{i=1}^{N_q} k_{j,i} q_i + \sum_{i,k=1}^{N_q} k_{j,i,k} q_i q_k + \sum_{i,k,l=1}^{N_q} k_{j,i,k,l} q_i q_k q_l = k_h \left(q_{\tilde{N}} \psi_j - \sum_{i=1}^{N_q} q_i \psi_i^2 \right) + c_h \left(\dot{q}_{\tilde{N}} \psi_j - \sum_{i=1}^{N_q} \dot{q}_i \psi_i^2 \right); \quad (14)$$

$$m_h \ddot{q}_{\tilde{N}} + c_h \left(\dot{q}_{\tilde{N}} - \sum_{i=1}^{N_q} \dot{q}_i \psi_i \right) + k_h \left(q_{\tilde{N}} - \sum_{i=1}^{N_q} q_i \psi_i \right) = A_h \sin(\Omega t) - m_h g; \quad (15)$$

where the modal mass of the plate is given by $m_j = \frac{1}{4} \rho a b h$; $c_{j,i}$ represents the linear modal damping coefficient of the plate; $k_{j,i}$, $k_{j,i,k}$, and $k_{j,i,k,l}$ are stiffness terms representing linear, quadratic, and cubic nonlinearities of the plate, respectively; $\psi_i(x_1, y_1)$ denotes the modal shape associated with the i -th generalized coordinate of the plate; $q_{\tilde{N}}$ is the generic term of the vector \mathbf{q} that refers to the generalized amplitude of the SMD model (w_h).

Equations (14) and (15) describe the dynamics of the contact phase, where the jumper is coupled to the plate. During this phase, the SMD model applies a reaction force to the plate, representing the dynamic interaction between the human and the structure. In this study, this force is labeled as the Plate Reaction Force (*PRF*). To account for the flight phase, i.e., the time when the jumper loses contact with the plate, *PRF* is assumed to be zero, and the only force acting on the SMD model is $G_h = m_h g$,

$$PRF = -c_h \left(\dot{q}_{\tilde{N}} - \sum_{i=1}^{\tilde{N}-1} \dot{q}_i \psi_i \right) - k_h \left(q_{\tilde{N}} - \sum_{i=1}^{\tilde{N}-1} q_i \psi_i \right). \quad (16)$$

During the flight phase (i.e., $PRF = 0$), the plate undergoes damped free vibration, and a decoupled system of nonlinear dynamic equilibrium equations can be derived. Thus, adapting (14) by neglecting the human

biodynamic parameters, the following can be obtained:

$$m_j \ddot{q}_j + \sum_{i=1}^{\tilde{N}-1} c_{j,i} \dot{q}_i + \sum_{i=1}^{\tilde{N}-1} k_{j,i} q_i + \sum_{i,k=1}^{\tilde{N}-1} k_{j,i,k} q_i q_k + \sum_{j,i,k,l=1}^{\tilde{N}-1} k_{j,i,k,l} q_i q_k q_l = 0; \quad (17)$$

Additionally, during the flight phase, the SMD model undergoes free fall motion, and its dynamic equation is decoupled from the plate, as shown by:

$$m_h \ddot{q}_{\tilde{N}} = -G_h. \quad (18)$$

Assuming $\alpha = -G_h/m_h$, the solutions to Eq. (18) for human displacements and velocities during the flight phase are expressed as follows:

$$q_{\tilde{N}}(t) = \frac{1}{2} \alpha t^2 + (\dot{q}_{\tilde{N}}(t_0) - \alpha t_0) t + \left(q_{\tilde{N}}(t_0) + \frac{1}{2} \alpha t_0^2 - t_0 \dot{q}_{\tilde{N}}(t_0) \right); \quad (19)$$

$$\dot{q}_{\tilde{N}}(t) = \alpha t + (\dot{q}_{\tilde{N}}(t_0) - \alpha t_0). \quad (20)$$

where the displacement response is modeled as a parabolic function, with t_0 denoting the initial time of the flight phase.

Consequently, two sets of nonlinear equations are derived for the studied problem. The first set, (12) and (13), describes the coupled interactions between the plate and the SMD during the contact phase. The second set encompasses the decoupled equations governing the dynamics of the unloaded plate (17) and the free-fall motion of the SMD model (19) and (20) during the flight phase. These sets are then solved as a piecewise-smooth contact dynamics problem [11, 14] and are numerically integrated using the Runge-Kutta fourth order method. In this process, *PRF* is controlled to accurately determine the touch-down ($PRF > 0$) and take-off ($PRF = 0$) events.

3 Numerical Results

The movement of the jumper is studied considering human-induced cyclic vibrations on a concrete rectangular plate. The plate has the following physical and geometrical properties: $a = 7.6$ m, $b = 7.6$ m, $h = 0.10$ m, $E = 23.94$ GPa, $\rho = 2500$ kg/m³, $\nu = 0.20$, and $\xi_p = 0.020$. These values were chosen such that the natural frequency of the plate matches the second harmonic of the jumper's frequency ($\frac{\omega_{1,1}}{\omega_h} = 2$). To model the simply supported plate with fixed edges, 16 degrees of freedom ($N_q = 16$) for the displacement fields (u , v , and w) in the expansions of Eq. (8), (9), and (10) were considered, as used in [12]. The SMD model is located at the mid-span of the plate ($x_1 = \frac{a}{2}$ and $y_1 = \frac{b}{2}$), with biodynamic properties given by: $m_h = 76.64$ kg and $\omega_h = 2.479$ Hz, resulting in a leg stiffness of $k_h = 18.6$ kN/m [4, 11]. For computational convenience, a nondimensionalization of variables is introduced, where time is scaled by the decoupled human body frequency ω_h , and both the plate vibration amplitude ($w_{1,1}$) and the displacement of the jumper's body center of mass (w_h) are divided by parameter $\eta = \frac{g}{\omega_h^2} = 0.04$ m. To understand the behavior of the system for a weakly damped jumper, a constant value of $\zeta_h = 0.1$ has been adopted for the numerical analyses. For the numerical integration of the piecewise-smooth contact dynamics system of nonlinear ordinary differential equations, a time-direct integration method is used.

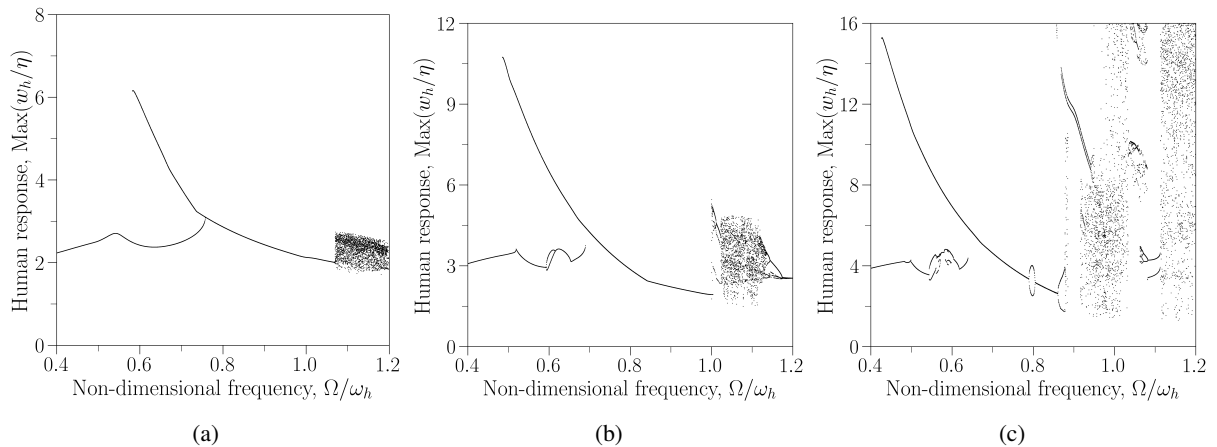


Figure 3. Frequency response curve of the SMD model for increasing forcing frequencies values with $\zeta_h = 0.1$ and (a) $A_h = 1.0 G_h$, (b) $A_h = 1.5 G_h$ and (c) $A_h = 2.0 G_h$.

Figure 3 displays the frequency-amplitude response for the displacement of the human center of mass for forcing frequency values ranging from $\Omega = 0.4\omega_h$ to $\Omega = 1.2\omega_h$, corresponding to values from 1.0 to 3.0 Hz. For the propulsion force amplitudes, the following values are investigated: $A_h = 1.0G_h$, $A_h = 1.50G_h$, and $A_h = 2.0G_h$, with $G_h = m_h g$. Figure 5a depicts that for $A_h = 1.0, G_h$, the jumper exhibits softening behavior with two 1T periodic jumping strategies when lower forcing frequency values are chosen: one at low amplitude and another at high amplitude. This indicates that the SMD model can converge to either bobbing or jumping behavior in a steady state, depending on the initial conditions, which is consistent with the experimental findings of [4] and [2]. Increasing the amplitude of the excitatory force, the low-amplitude solution transitions to a periodic 2T solution and subsequently to a 4T solution at the same frequency point, as illustrated in Fig.5b and 5c, respectively. At higher excitation frequencies, windows of chaotic solutions can be observed, indicating the difficulty of jumping periodically on the floor. This transition of periodicity is confirmed by the phase portraits and Poincaré maps shown in Fig. 4.

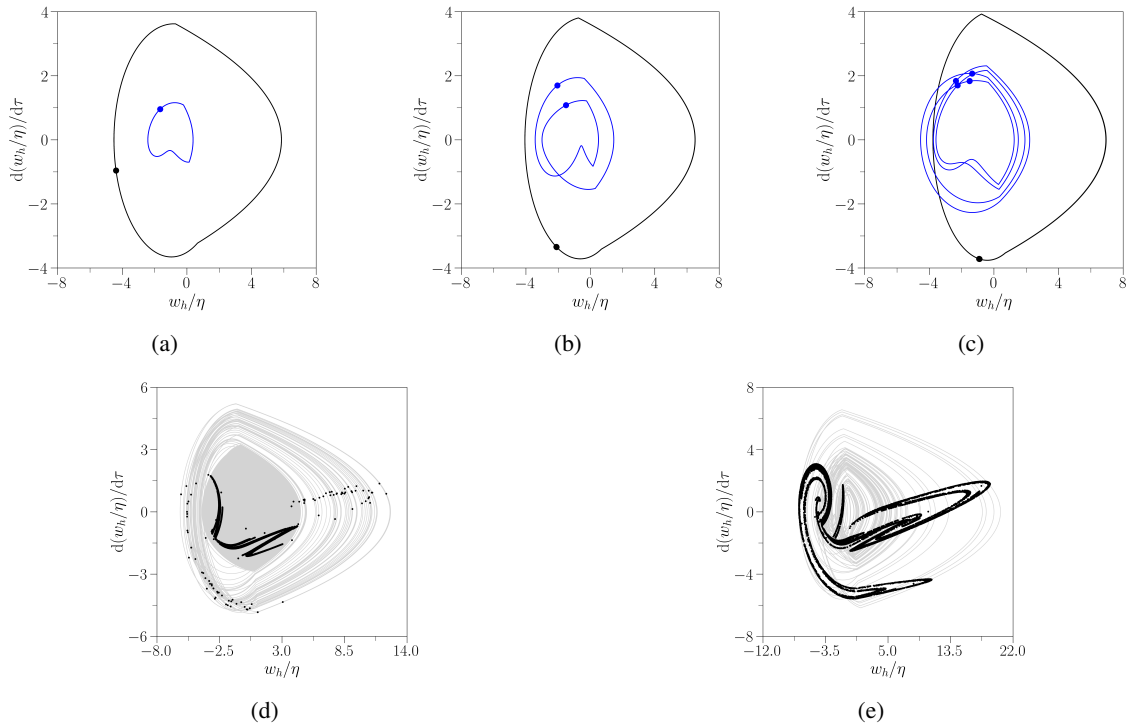


Figure 4. Phase portraits and Poincaré maps of human response with $\zeta_h = 0.1$ for (a) $\Omega = 0.60\omega_h$ and $A_h = 1.00G_h$ (b) $\Omega = 0.60\omega_h$ and $A_h = 1.5G_h$ (c) $\Omega = 0.60\omega_h$ and $A_h = 2.00G_h$ (d) $\Omega = 1.1\omega_h$ and $A_h = 1.50G_h$ (e) $\Omega = 1.00\omega_h$ and $A_h = 2.00G_h$

The dynamic response of the plate under human excitation was also investigated. Obtained results showed that, even with the decoupling during jumps, and considering the evaluated mass and frequency ratio between the structure and the jumper, the SMD model significantly influenced the mechanical behavior of the plate, acting as a tuned mass damper (TMD). This was evidenced by the splitting of the resonance peak into two, due to the coupling of the SMD model's vibration modes with those of the structure, creating two new resonance frequencies close to the original one and redistributing the vibrational energy between them, as shown in Fig. 5a. As the propulsion force (A_h) exerted on the plate increases, more resonance peaks emerge due to nonlinear interactions and more complex dynamic coupling, as seen in Figs. 5b and 5c.

4 Concluding Remarks

In this work the dynamic interaction between a human jumper and a concrete rectangular plate under cyclic vertical jumps is analyzed. The mechanical system is described by a set of piecewise smooth-touch nonlinear differential equations, allowing for the consideration of contact loss between the jumper and the plate during jumps. The analyses demonstrated that the jumper exhibits complex dynamics, including periodic and chaotic responses, depending on parameter combinations for the system. The results highlight that the SMD model also can affect the mechanical behavior of the plate, due to the coupling of the jumper's vibration modes with the structure's, creating new resonance frequencies and redistributing vibrational energy.

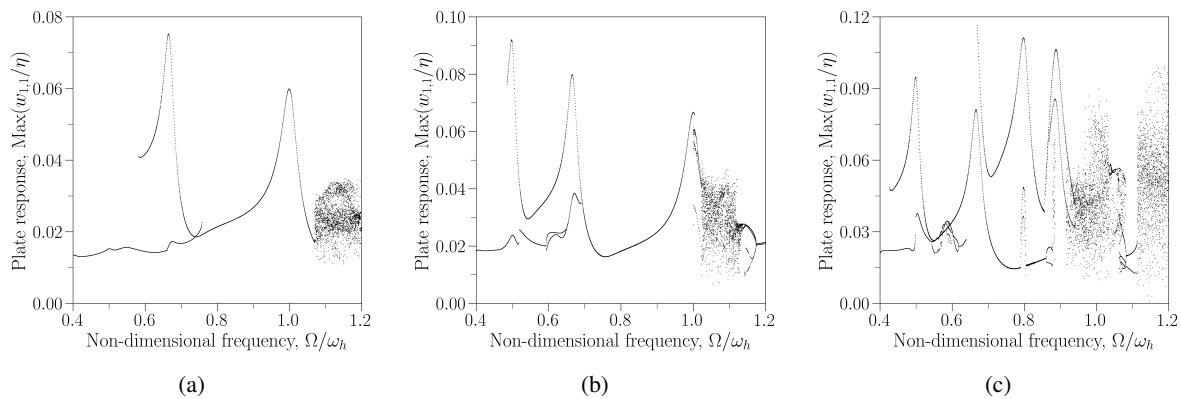


Figure 5. Frequency response curve of the plate for increasing forcing frequencies values with $\zeta_h = 0.1$ and (a) $A_h = 1.0 G_h$, (b) $A_h = 1.5 G_h$ and (c) $A_h = 2.0 G_h$.

Acknowledgements. This work was made possible by the support of the Coordination of Higher Level Personal Improvement – CAPES and Federal University of Goiás computational laboratories.

Authorship statement. The authors hereby confirm that they are the sole liable persons responsible for the authorship of this work, and that all material that has been herein included as part of the present paper is either the property (and authorship) of the authors, or has the permission of the owners to be included here.

References

- [1] E. Shahabpoor, A. Pavic, and V. Racic. Interaction between walking humans and structures in vertical direction: A literature review. *Shock and vibration*, vol. 2016, 2016.
- [2] R. E. White, J. H. Macdonald, T. R. Horseman, and N. A. Alexander. Exploring interactions between a human rhythmic jumper and an oscillating structure using experimental force–displacement analysis. *Structures*, vol. 51, pp. 1172–1188, 2023.
- [3] C. M. R. Gaspar. *Avaliação do efeito da interação humana sobre pisos de edificações submetidos a atividades humanas rítmicas*. PhD thesis, Universidade do Estado do Rio de Janeiro, 2018.
- [4] R. E. White, J. H. Macdonald, and N. A. Alexander. A nonlinear frequency-dependent spring-mass model for estimating loading caused by rhythmic human jumping. *Engineering Structures*, vol. 241, pp. 112229, 2021a.
- [5] Y. El Asri, M. Couchaux, M. Hjjaj, and M. Lukić. Spectral modelling approach for crowd-rhythmic activities performed on steel-concrete composite floors. *Engineering Structures*, vol. 299, pp. 117066, 2024.
- [6] M. S. Pfeil, W. D. Varela, and da N. d. P. A. Costa. Experimental calibration of a one degree of freedom biodynamic model to simulate human walking-structure interaction. *Engineering Structures*, vol. 262, pp. 114330, 2022.
- [7] C. Gaspar, E. Caetano, C. Moutinho, and J. G. S. Silva. Active human-structure interaction during jumping on floors. *Structural Control and Health Monitoring*, 2019.
- [8] S. Yao, J. Wright, A. Pavic, and P. Reynolds. Experimental study of human-induced dynamic forces due to jumping on a perceptibly moving structure. *Journal of Sound and Vibration*, vol. 296, n. 1-2, pp. 150–165, 2006.
- [9] R. Harrison, S. Yao, J. Wright, A. Pavic, and P. Reynolds. Human jumping and bobbing forces on flexible structures: effect of structural properties. *Journal of engineering mechanics*, vol. 134, n. 8, pp. 663–675, 2008.
- [10] V. Racic, J. Brownjohn, and A. Pavic. Reproduction and application of human bouncing and jumping forces from visual marker data. *Journal of Sound and Vibration*, vol. 329, n. 16, pp. 3397–3416, 2010.
- [11] R. E. White, N. A. Alexander, J. H. Macdonald, and A. R. Champneys. Parametric exploration of a simple model of human jumping on an oscillating structure. *Journal of Sound and Vibration*, vol. 509, pp. 116227, 2021b.
- [12] P. V. I. Dias and Z. J. G. N. Del Prado. Human-structure interaction during jumping on rectangular plates. In *XLIII Ibero-Latin American Congress on Computational Methods in Engineering*, volume 4, 2022.
- [13] M. Amabili. *Nonlinear vibrations and stability of shells and plates*. Cambridge University Press, 2008.
- [14] M. Bernardo, C. Budd, A. R. Champneys, and P. Kowalczyk. *Piecewise-smooth dynamical systems: theory and applications*, volume 163. Springer Science & Business Media, 2008.